Ras inhibitors display an anti-metastatic effect by downregulation of lysyl oxidase through inhibition of the Ras-PI3K-Akt-HIF-1α pathway

Yoshikawa, Yoko ; Takano, Osamu ; Kato, Ichiro ; Takahashi, Yoshihisa ; Shima, Fumi ; Kataoka, Tohru

(Citation)
Cancer Letters,410:82-91

(Issue Date)
2017-12-01

(Resource Type)
journal article

(Version)
Accepted Manuscript

(URL)
https://hdl.handle.net/20.500.14094/90004440

Ras Inhibitors Display an Anti-Metastatic Effect by Downregulation of Lysyl Oxidase through Inhibition of the Ras-PI3K-Akt-HIF-1α Pathway

Yoko Yoshikawa[1], Osamu Takano[1], Ichiro Kato[1], Yoshihisa Takahashi[1], Fumi Shima[2]*, and Tohru Kataoka[1]*

Affiliations

[1]Division of Molecular Biology, Department of Biochemistry and Molecular Biology, Kobe University Graduate School of Medicine, Kobe 650-0017, Japan.

[2]Drug Discovery Science, Division of Advanced Medical Science, Department of Science, Technology and Innovation, Kobe University Graduate School of Science, Technology and Innovation, Kobe 650-0017, Japan.

***Corresponding authors**

Tohru Kataoka, MD, PhD

Division of Molecular Biology, Department of Biochemistry and Molecular Biology, Kobe University Graduate School of Medicine, 7-5-1 Kusunoki-cho, Chuo-ku, Kobe 650-0017, Japan.

Tel: +81-78-382-5380, Fax: +81-78-382-5399, E-mail: kataoka@people.kobe-u.ac.jp

Fumi Shima, MD, PhD

Drug Discovery Science, Division of Advanced Medical Science, Department of Science, Technology and Innovation, Kobe University Graduate School of Science, Technology and Innovation, 7-5-1 Kusunoki-cho, Chuo-ku, Kobe 650-0017, Japan.

Tel: +81-78-382-6033, Fax: +81-78-382-6034, E-mail: sfumi@med.kobe-u.ac.jp

Abstract (184/185 words)

Metastasis stands as the major obstacle for the survival from cancers. Nonetheless most existing anti-cancer drugs inhibit only cell proliferation, and discovery of agents having both anti-proliferative and anti-metastatic properties would be more beneficial. We previously reported the discovery of small-molecule Ras inhibitors, represented by Kobe0065, that displayed anti-proliferative activity on xenografts of human colorectal cancer (CRC) cell line SW480 carrying the K-*ras*^{G12V}gene. Here we show that treatment of cancer cells carrying the activated *ras* genes with Kobe0065 or an siRNA targeting Ras downregulates the expression of lysyl oxidase (LOX), which has been implicated in metastasis. LOX expression is enhanced by co-expression of Ras^{G12V} through activation of phosphatidylinositol 3-kinase (PI3K)/Akt and concomitant accumulation of hypoxia-inducible factor (HIF)-1α. Furthermore, Kobe0065 effectively inhibits not only migration and invasion of cancer cells carrying the activated *ras* genes but also lung metastasis of human CRC cell line SW620 carrying the K-*ras*^{G12V} gene. Collectively, these results indicate that Kobe0065 prevents metastasis through inhibition of the Ras-PI3K-Akt-HIF-1α-LOX signaling and suggest that Ras inhibitors in general might exhibit both anti-proliferative and anti-metastatic properties toward cancer cells carrying the activated *ras* genes.

Keywords: metastasis; Ras; Ras inhibitors; LOX; PI3K; HIF-1α

Abbreviations: CRC, colorectal cancer; LOX, lysyl oxidase; PI3K, phosphatidylinositol 3-kinase; HIF, hypoxia-inducible factor; GEF, guanine nucleotide exchange factor; GAP, GTPase-activating protein; ECM, extracellular matrix; mTOR, mammalian target of rapamycin; β-APN, 3-aminopropionitrile fumarate salt; DMSO, dimethyl sulfoxide; GAPDH, glyceraldehyde-3-phosphate dehydrogenase; FBS, fetal bovine serum; DMEM, Dulbecco's modified Eagle's medium; 2D, two-dimensional; 3D, three-dimensional; siRNA, small interfering RNA; H&E, hematoxylin & eosin; qRT-PCR, quantitative

reverse transcription-polymerase chain reaction; EMT, epithelial-mesenchymal transition.

1. Introduction

The *ras* oncogene products (H-Ras, K-Ras and N-Ras) function as binary switches by cycling between GTP-bound (Ras•GTP) active and GDP-bound (Ras•GDP) inactive forms and play pivotal roles in controlling cell proliferation and differentiation [1]. Interconversion between the two forms is catalyzed by guanine nucleotide exchange factors (GEFs) or GTPase-activating proteins (GAPs) [2]. Ras•GTP interacts directly with its downstream effectors including Raf kinases and phosphatidylinositol 3-kinases (PI3Ks) for exerting its diverse growth-stimulating functions [1, 2]. Since mutational activation of Ras is observed in 15~20% of human cancers, specifically in 60~90% of pancreatic and 30~50% of colorectal carcinomas (CRCs) [1, 3, 4], agents directly inhibiting Ras are presumed to become promising anti-cancer drugs. We succeeded in the discovery of small-molecule Ras inhibitors, Kobe0065-family compounds, that blocked the interactions of Ras•GTP with its effectors and displayed anti-proliferative activity toward xenografts of human CRC cell line SW480 carrying the K-ras^{G12V} [5].

Various factors are involved in tumor progression and malignant transformation. In particular, invasion and metastasis of cancer cells represent one of the major causes of poor survival, the inhibition of which is one of the targets for anti-cancer drug development [6-8]. It has been reported that lysyl oxidase (LOX) is closely related to tumor progression and metastasis under hypoxia [9, 10]. LOX, a member of the multigene family consisting of at least five constituents, is a secreted amine oxidase that modifies primary tumor microenvironment by crosslinking collagens and elastins in the extracellular matrix (ECM) [11, 12]. LOX is initially synthesized as an inactive 46-kDa preproenzyme, prepro-LOX, and the 21-amino acid signal peptide is cleaved during biosynthesis [13]. The resulting propeptide is glycosylated to yield 50-kDa pro-LOX and subsequently secreted into the ECM. Thereafter, pro-LOX is proteolytically cleaved by procollagen C-proteinase, yielding the 32-kDa active mature enzyme, mature-LOX [13]. LOX was reported to be involved in the metastasis of CRC cells such as SW480 and its patient-matched metastatic clone, SW620 [14, 15]. The expression of LOX is enhanced by the

activation of PI3K/Akt [16-18], downstream molecules of Ras, and targeted by hypoxia-inducible factor (HIF)-1, a transcription factor composed of α and β subunits [9, 19]. The stability of the α subunit is regulated by cellular oxygen levels while the β subunit is constitutively expressed [19]. Activation of PI3K/Akt enhances the production of HIF-1α via phosphorylation and activation of mammalian target of rapamycin (mTOR) [20, 21] . In addition, Ras were implicated in regulation of HIF-1α activation although the underlying mechanism was unclear [22-25].

In this study, we investigate the role of Ras signaling in not only the regulation of LOX expression and HIF-1α activation but also the metastatic properties of cancer cells by using the Kobe0065-family compounds [5] and find that the compounds prevent metastasis through inhibition of the Ras-PI3K-Akt-HIF-1α-LOX signaling. These results suggest that Ras inhibitors in general may exhibit an anti-metastatic activity toward cancer cells carrying the activated *ras* mutations adding to an anti-proliferative activity.

2. Materials and Methods

2.1 Reagents

Kobe0065 and sorafenib were obtained as described before [5]. LY294002, 3-aminopropionitrile fumarate salt (β-APN) and Chrysin were obtained from Millipore (Billerica, MA, USA), SIGMA-Aldrich (St. Lois, MO, USA) and Santa Cruz Biotech. (Santa Cruz, CA, USA), respectively. For *in vitro* experiments, all the compounds were dissolved in dimethyl sulfoxide (DMSO). For *in vivo* experiments, the compounds were suspended in Cremophore EL:ethanol:water = 1:1:6. Anti-LOX antibodies were purchased from Abnova (Taipei, Taiwan) and Santa Cruz Biotech. Antibodies against glyceraldehyde-3-phosphate dehydrogenase (GAPDH), H-Ras (C-20), K-Ras (F-234) and HIF-1α (H–206) were purchased from Santa Cruz Biotech. Antibodies against phosphorylated Akt and total Akt were purchased from Cell Signaling (Danvers, MA, USA). Horseradish peroxidase-conjugated secondary

antibodies against rabbit and mouse immunoglobulin Gs were purchased from GE Healthcare (Buckinghamshire, UK).

2.2 Cell lines

Mouse fibroblast NIH3T3 carrying the wild-type *ras*, human metastatic CRC SW620 carrying the K-*ras*^{G12V}, human pancreatic cancers Panc-1 carrying the K-*ras*^{G12D} and BxPC-3 carrying the wild-type *ras* and human breast cancer MCF-7 carrying the wild-type *ras* and the constitutively activated *pik3ca*^{E545K} were obtained from the European Collection of Cell Cultures. NIH3T3 cells stably expressing H-Ras^{G12V} or c-Raf-1$^{S259A,\ Y340D,\ Y341D}$ were described before [5]. SW620 cells were maintained in L-15 medium (GIBCO, Grand island, NY, USA) containing 10% fetal bovine serum (FBS) (Nichirei Biosciences Inc., Tokyo, Japan). The other cell lines were maintained in Dulbecco's modified Eagle's medium (DMEM) (Nakalai Tesque, Kyoto, Japan) containing 10% FBS.

2.3 Cell culture and compound treatment

For two-dimensional (2D) cell culture, 1×10^7 cells seeded on a 10 cm-dish were treated with 20 μM Kobe0065, 50 μM LY294002 or DMSO in the presence of 10% FBS for 24 h at 37 °C. Thereafter, the FBS concentration was reduced to 2% and the cells were further incubated for 3 h. For three-dimensional (3D) cell culture, 1×10^5 cells were suspended in 40 μl of medium containing 20 μM Kobe0065, 50 μM LY294002, 300 μM β-APN, 30 μM Chrysin or DMSO in the presence of 10% FBS, seeded on each well of *PrimeSurface*® 96-well plates (Sumitomo Bakelite Co., Ltd., Tokyo, Japan) and cultured for 24 h at 37 °C. Thereafter, 160 μl of FBS-free medium containing the equal concentration of the compound was added to each well to adjust the final FBS concentration to 2 % and further incubated for 3 h.

2.4 Animal models and drug administration

Female athymic nude (nu/nu) mice (6-8 weeks old) were obtained from CLEA Japan, Inc. All the animals were maintained at the animal facilities of Kobe University Graduate School of Medicine. The use and care of the animals were reviewed and approved by the Institutional Animal Care and Use Committee of Kobe University. For an experimental lung metastasis model, nude mice were orally administered with the compounds for 5 days. Subsequently, 1×10^7 SW620 cells suspended in 200 μl L-15 medium were injected via tail vein, and the oral administration was continued for further 8 weeks.

2.5 Small interfering RNA (siRNA)-mediated gene silencing

Cells were transfected with 3 sets of the Stealth™ siRNAs against human LOX, human K-Ras or non-targeting control (Invitrogen, Carlsbad, CA, USA) by using Lipofectamine RNAiMAX (Invitrogen) according to the manufacturer's instructions. After transfection, the cells were cultured for 24 h at 37 °C and subjected to further experiments. The Stealth™ siRNAs were listed in supplementary Table 1.

2.6 Wound healing migration assay

After the siRNA treatment, 5×10^6 cells, which reached confluency in 12-well plates, were treated with 20 μM Kobe0065, 300 μM β-APN or DMSO in the presence of 5% FBS and a "wound" was inflicted on the cells in each well by scratching with a 200 μl-pipet tip. In 24 h for SW620 and Panc-1 and 48 h for BxPC-3, the cells migrated into the wounded area were observed under a microscope.

2.7 Anchorage-dependent proliferation assay

After the siRNA treatment, the cells were seeded on 96-well plates (6,000 cells for SW620 and 3,000 cells for Panc-1 and BxPC-3 per well) and treated with 20 μM Kobe0065 or DMSO in the presence of 5% FBS for 72 h. Cell viability was determined by the addition of Cell Counting Reagent (Nakalai Tesuque) according to the manufacturer's instruction.

2.8 Invasion assay

After serum-deprivation for 24 h, 5×10^4 cells suspended in FBS-free DMEM containing Kobe0065 or DMSO were seeded in triplicate on BD BioCoat™ Matrigel™ invasion chambers (BD Biosciences, MA, USA), transferred onto wells containing 10% FBS as a chemo-attractant, and incubated for 24 h at 37 °C. Thereafter, the chambers were wiped out of matrigel, and the membranes (8-μm pore size) were stained with hematoxylin for counting the number of the invaded cells.

2.9 RNA isolation and quantitative reverse transcription-polymerase chain reaction (qRT-PCR)

Total cellular RNAs from cultured cells and tissues were isolated by using Trizol (Invitrogen) and RNeasy Mini Kit (Qiagen), respectively. Total RNAs from paraffin-embedded tissue sections were isolated by using High Pure FFPET RNA Isolation Kit (Roche, Mannheim, Germany). All the procedures were carried out according to the manufacturers' instructions. QRT-PCR was carried out by using SYBR Premix Ex Taq II Kit (Takara Bio, Kyoto, Japan) with Thermal Cycler Dice Real Time System (Takara Bio). Relative mRNA levels were determined by the comparative *Ct* method, followed by normalization with the *GAPDH* or *β-actin* mRNA levels. The primers are listed in supplementary Table 2.

2.10 Western blot

After treatment with siRNA or compounds, cells were solubilized, separated by SDS-PAGE and subjected to immunoblotting as described previously [26].

2.11 Immunoprecipitation of secreted-LOX in culture medium

NIH3T3 cells stably expressing H-Ras^{G12V} were treated with 20 μM Kobe0065 or DMSO in 3D

culture. Thereafter, the culture medium was subjected to immunoprecipitation by an anti-LOX antibody (Santa Cruz Biotech.) and protein A-Sepharose resin at 4 °C overnight. After washing the resin twice with PBS, proteins bound to the resin were separated by SDS-PAGE and subjected to the detection of LOX by using another anti-LOX antibody (Abnova).

2.12 Evaluation of lung metastasis

Dissected lungs were fixed in 4% paraformaldehyde, embedded in paraffin and subjected to hematoxylin & eosin (H&E) staining. For histological evaluation of lung micro-metastasis, the number of micro-metastatic nodules in three non-continuous lung sections from each mouse was counted under a light microscope. Immunohistochemical detection of LOX in the paraffin-embedded lung sections was performed as described in [5].

2.13 Statistics

The values were presented as the mean ± SEM. Statistical significance for groups of three or more was determined by one way analysis of variance (ANOVA). Differences were considered to be statistically significant when the p value was less than 0.05. *, $p<0.05$; **, $p<0.01$; and ***, $p<0.001$.

3. Results

3.1 LOX expression is upregulated by Ras activation and downregulated by treatment with an siRNA against Ras or Kobe0065.

We first examined the effect of Kobe0065, the most potent inhibitor among the Kobe0065-family compounds [5], on LOX expression in three human cancer cell lines, SW620 carrying the K-ras^{G12V}, Panc-1 carrying the K-ras^{G12D} and BxPC-3 carrying the wild-type *ras* in 2D culture. These cell lines showed high expression of 46-kDa prepro-LOX, which was effectively downregulated by treatment with

20 μM Kobe0065 in SW620 and Panc-1 but not BxPC-3 (Fig. 1A). We next examined the effect of the siRNA-mediated K-Ras knockdown on LOX expression. Treatment with K-Ras siRNA or Kobe0065 inhibited the LOX expression in SW620 and Panc-1 cells but not BxPC-3 cells at both the mRNA and protein levels, while LOX siRNA treatment inhibited the LOX expression in all the cell lines (Fig. 1B and C). We also observed a similar reduction in the LOX expression by K-Ras siRNA and Kobe0065 in these cell lines grown in 3D culture (Fig. 1D, E). Also, treatment with the other Kobe0065-family compounds, Kobe2601 and Kobe 2602 [5], inhibited the LOX expression in SW620 grown in 3D culture (Fig. S1). Next, we examined the effect of the overexpression of H-Ras^{G12V} on LOX expression in NIH3T3 cells. When grown in 2D culture, NIH3T3 cells stably expressing H-Ras^{G12V} failed to show any changes in the *LOX* mRNA level compared to the parental cells (Fig. 1F). However, when grown in 3D culture, an increase in the *LOX* mRNA level was observed depending on the H-Ras^{G12V} expression, which was reduced to the basal level by Kobe0065 treatment. Western blot analysis showed that the cellular level of prepro-LOX was elevated in H-Ras^{G12V}-expressing cells grown in 3D culture but not 2D culture, which was also reduced to the basal level by Kobe0065 treatment (Fig. 1G). Likewise, the level of 32-kDa secreted mature-LOX was reduced by Kobe0065 treatment in the 3D culture medium of H-Ras^{G12V}-expressing cells (Fig. 1H). These findings suggested that LOX expression was upregulated by Ras activation.

3.2 Ras regulates LOX expression through activation of the PI3K-Akt pathway

To clarify the signaling pathway responsible for the Ras-dependent LOX expression, we examined the role of PI3K/Akt because it had been implicated in upregulation of LOX expression [16-18]. In SW620 cells grown in 3D culture, the *LOX* mRNA level was reduced by the treatment with a PI3K inhibitor, LY294002, to the level attained by the treatment with Kobe0065 or K-Ras siRNA (Fig. 2A). Western blot analysis showed that these treatments also inhibited the prepro-LOX expression and the

Akt phosphorylation (Fig. 2B). Likewise, SW620 cells grown in 2D culture showed a similar property (Fig. S2). In contrast, Kobe0065 treatment failed to inhibit the prepro-LOX expression and the Akt phosphorylation in MCF-7 cells carrying the wild-type *ras* and the constitutively activated *pik3ca*^{E545K}, suggesting that Ras drive the PI3K/Akt activation to upregulate the LOX expression (Fig. 2C). Likewise, NIH3T3 cells stably expressing H-Ras^{G12V} grown in 3D culture showed that the H-Ras^{G12V}-dependent increase in the *LOX* mRNA and prepro-LOX levels and the Akt phosphorylation was abrogated by the treatment with either Kobe0065 or LY294002 (Fig. 2D and E). We next examined the possible role of another Ras effector molecule, c-Raf-1, in LOX expression. Expression of a constitutively activated mutant of c-Raf-1, c-Raf-1$^{S259A, Y340D, Y341D}$, in NIH3T3 cells failed to elevate the *LOX* mRNA expression (Fig 2F). Moreover, treatment with sorafenib, an inhibitor of multiple protein kinases including Raf, failed to reduce the LOX expression (Fig. S1). Furthermore, we examined the effect of other small GTPases: M-Ras, Rap2A, RhoA and RalA, on LOX expression because Kobe0065 had been suggested to interact with them [5]. The overexpression of M-Ras^{Q71L}, Rap2A^{G12V}, RhoA^{G14V} or wild-type RalA had no effect on the *LOX* mRNA levels (Fig. S3). These results, taken together, indicated that the Ras-PI3K-Akt signaling pathway was mainly responsible for the LOX upregulation.

3.3 Ras regulates LOX expression through PI3K/Akt-mediated HIF-1α accumulation

During normoxia, HIF-1α is hydroxylated by prolyl hydroxylases, which enables it to interact with ubiquitin ligases, leading to the ubiquitylation and subsequent degradation in proteasomes [21]. Hypoxia prevents the ubiquitylation of HIF-1α and leads to the accumulation in the cytoplasm, thereby causing its nuclear translocation to enhance the expression of the target genes such as *LOX* [27]. Recently, it had been reported that activation of the PI3K-Akt signaling enhances the stabilization of HIF-1α [16, 17]. This led us to examine the role of HIF-1α in LOX upregulation via the Ras-PI3K-Akt pathway. In SW620 cells grown in 3D culture, the siRNA-mediated K-Ras knockdown as well as the treatment with

Kobe0065 or LY294002 reduced the amount of HIF-1α at the protein level but not the mRNA level and the phosphorylation level of Akt (Fig. 3A and B). Also, the treatments with Kobe0065 and K-Ras siRNA reduced the HIF-1α accumulation and the Akt phosphorylation in Panc-1 cells but not in BxPC-3 cells (Fig. S4). Likewise, in NIH3T3 cells stably expressing H-Ras^{G12V} grown in 3D culture, H-Ras^{G12V} expression increased the HIF-1α protein level, which was abrogated by the treatment with Kobe0065 or LY294002, while the *HIF-1α* mRNA level remained unaffected (Fig. 3C and D). β-APN, an irreversible inhibitor of the LOX catalytic activity, failed to show any effects on either HIF-1α or prepro-LOX levels (Fig. 3B and D), while Chrysin [28], an inhibitor of HIF-1α expression, reduced both the HIF-1α and prepro-LOX levels without affecting the *HIF-1α* mRNA levels (Fig. 3E and F), indicating that LOX functions downstream of HIF-1α. Moreover, treatment with β-APN or Chrysin failed to affect the Akt phosphorylation (Fig. 3B, D, and F). Taken together, these results indicated that the Ras-PI3K-Akt signaling caused the HIF-1α accumulation, thereby inducing the LOX expression.

3.4 Effects of Kobe0065 treatment on migration and invasion of cancer cells.

We next examined the effect of Kobe0065 on migration and invasion of cancer cell lines, which were relevant to their metastatic ability. Treatment with LOX siRNA or β-APN inhibited the migration of SW620, Panc-1 and BxPC-3 as shown by the wound healing migration assay (Fig. 4A), indicating that LOX played a crucial role in regulation of the cell migration. In contrast, treatment with K-Ras siRNA or Kobe0065 markedly attenuated the migration of SW620 and Panc-1 cells but not BxPC-3 cells. On the other hand, these treatments failed to inhibit the anchorage-dependent proliferation under the same culture condition containing 5% FBS as that used in the migration assay (Fig. 4B), indicating that their migration inhibitory effect was not ascribable to the anti-proliferative activity. The failure to inhibit proliferation at high FBS concentrations was consistent with our previous observation that Kobe0065 exhibited an anti-proliferative activity only at low FBS concentrations [5] and presumably

accounted for by activation of Ras effectors such as Raf kinases via Ras-independent pathways such as that involving protein kinase C, *etc*. On the other hand, Kobe0065 treatment exhibited a dose-dependent inhibition of the cellular invasion of SW620 and Panc-1 cells but not BxPC-3 cells as tested by the Matrigel™ invasion assay (Fig. 5A and B). These results collectively suggested the crucial role of Ras in controlling the migration and invasion of cancer cells carrying the activated *ras* genes.

3.5 Kobe0065 prevents lung metastasis of human CRC cells carrying the activated *ras* genes.

The results described above prompted us to evaluate the anti-metastatic activity of Kobe0065 in the mouse experimental model of lung metastasis using injection of SW620 cells via tail vein. Histological analyses of the lung tissues showed that only 3 mice out of 4 and 3 mice out of 6 developed metastatic tumor nodules after 8-weeks administration with 80 and 160 mg/kg Kobe0065, respectively, whereas all of 7 control mice developed metastatic tumors in their lungs (Fig. 6A and B). Also, the numbers of the metastatic nodules per lung were substantially diminished by Kobe0065 treatment (Fig. 6C), whereas administration of 80 mg/ml sorafenib failed to inhibit the lung metastasis (Fig. 6A-C). Moreover, the *LOX* mRNA levels in the lung sections were substantially reduced by treatment with Kobe0065 in a dose-dependent manner but not with sorafenib (Fig. 6D). Immunohistochemical analysis showed elevated expression of LOX in the metastatic nodules, which was inhibited by administration of Kobe0065 but not sorafenib (Fig. 6E).

4. Discussion

In this study, we presented a series of experimental evidence showing that Ras activation upregulated LOX expression through activation of the PI3K-Akt-HIF-1α pathway and that treatment with a Ras inhibitor, exemplified by Kobe0065, effectively suppressed not only migration and invasion but also lung metastasis of human cancer cell lines carrying the activated *ras* genes via downregulation of the

LOX expression. We did not observe any effects of Kobe0065 treatment on the mRNA levels of the 4 other LOX family members by microarray analysis (data not shown). Our result that the activation of the PI3K-Akt signaling enhanced the accumulation of HIF-1α at the protein level but not the mRNA level (Fig. 3) is consistent with the reported mechanism where the activated Akt enhances the production of HIF-1α via phosphorylation and activation of mTOR, which phosphorylates and activates S6 kinase thereby facilitating the translation of the *HIF-1α* mRNA [20, 21]. Although activation of ERK downstream of the Ras-Raf signaling was reported to upregulate HIF-1α expression leading to the induction of vascular endothelial growth factor [29], our result that neither constitutively activated c-Raf (Fig. 2F) nor sorafenib (Fig. S1) affected LOX expression excluded the possibility of the involvement of ERK. Our results also showed that the enhanced expression of LOX downstream of the PI3K-Akt-HIF-1α signaling was necessary for migration and invasion of cancer cells carrying the activated *ras* genes. It is well recognized that the PI3K-Akt signaling plays critical roles in metastasis of cancer cells by promoting cellular events such as invasion, migration and epithelial-mesenchymal transition (EMT) via activation of the transcription factors, Twist and Snail, and inhibition of GSK-3β [30-32]. Our results implied that LOX also plays a critical role in metastasis working in parallel with these known PI3K-Akt target proteins. We did not observe any inhibitory effects of Kobe0065 or K-Ras siRNA on LOX expression (Fig. 1), Akt activation (Fig. 2C), HIF-1α accumulation (Fig. S4), migration (Fig. 4) and invasion (Fig. 5) in cells carrying the wild-type *ras* genes. This may be accounted for lower dependence of PI3K activation on Ras in these cells because PI3K isoforms are also activated by other regulators including heterotrimeric G proteins [33].

We observed that NIH3T3 cells stably expressing H-Ras^{G12V} failed to show elevated LOX expression in 2D culture (Fig. 1F and G) while cancer cell lines expressing K-Ras^{G12V} or K-Ras^{G12D} showed it in both 2D and 3D culture. This might be accounted for by the failure of NIH3T3 cells to reconstitute the surrounding ECM, which constitutes a 3D structure and is known to be hardly reproduced in cells grown

in 2D culture [11, 34-36]. In addition, expression of an ECM enzyme such as LOX was shown to be enhanced by culturing cells in 3D condition [37], which could be partly accounted for by the fact that a gradient of oxygen tension is created in 3D culture, forming a relatively hypoxic milieu in the central area of the 3D cellular bulk [38]. This may partly account for the difficulty in detecting LOX expression in 2D culture compared to 3D culture. Ras activation was reported to drive tumor progression with mitochondrial dysfunction thereby recapitulating hypoxic metabolism [39-41], which may further enhance HIF-1α accumulation and LOX expression synergistically with the activation of the PI3K-Akt signaling.

In this paper, we showed that Ras activation plays a crucial role in metastasis of cancer cells carrying the activated *ras* genes by enhancing LOX expression via activation of the PI3K-Akt-HIF-1α pathway. Furthermore, we showed that the Ras inhibitor Kobe0065 exhibited an anti-metastatic activity toward cancer cells carrying the activated *ras* genes. Our results suggest that Ras inhibitors in general may have both anti-proliferative and anti-metastatic properties, which would be more beneficial for the treatment of cancer patients than existing anti-cancer drugs inhibiting only cell proliferation. (total 3484/3500 words)

Acknowledgements

This work was supported by grants from the Princes Takamatsu Cancer Research Fund (grant number 13-24510), the National Institute of Biomedical Innovation (NIBIO) (grant number 06-3), the Ministry of Health, Labor and Welfare and Japan Agency for Medical Research and Development (AMED) (grant number 15ak0101006h0005), and NIBIO and AMED (grant number 15nk0101401h0002); and by MEXT/JSPS Kakenhi (grant number 26293026 and 26293065). We thank Dr. Masahiro Neya for the synthesis of the compounds used in this study.

Author contributions

TK supervised the study; YY, FS and TK conceived and designed experiments; YY, OT, IK and YT performed experiments; YY, OT and IK analyzed data; YY, FS and TK wrote the manuscript.

Conflict of interest

The authors declare no conflict of interest.

References

[1] Karnoub AE, Weinberg RA. Ras oncogenes: split personalities. *Nat Rev Mol Cell Biol* 2008; 9: 517-531.

[2] Vetter IR, Wittinghofer A. The guanine nucleotide-binding switch in three dimensions. *Science* 2001; 294: 1299-1304.

[3] Almoguera C, Shibata D, Forrester, K, Martin J, Arnheim N, Perucho M. Most human carcinomas of the exsocrine pancreas contain mutant c-K-*ras* genes. *Cell* 1988; 53: 549-554.

[4] Forrester K, Almoguera C, Han K, Grizzle WE, Perucho M. Detection of high incidence of K-ras oncogenes during human colon tumorigenesis. *Nature* 1987; 327: 298-303.

[5] Shima F, Yoshikawa Y, Ye M, Araki M, Matsumoto S, Liao J, et al. In silico discovery of small-molecule Ras inhibitors that display antitumor activity by blocking the Ras-effector interaction. *Proc Natl Acad Sci U S A* 2013; 110: 8182-8187.

[6] Fidler IJ. The pathogenesis of cancer metastasis: the 'seed and soil' hypothesis revisited. *Nat Rev Cancer.* 2003; 3(6): 453-8.

[7] Gupta GP, Massagué J. Cancer metastasis: building a framework. *Cell* 2006; 1 27(4): 679-95.

[8] Mack GS, Marshall A. Lost in migration. *Nat Biotechnol* 2010; 28: 214-229.

[9] Erler JT, Bennewith KL, Nicolau M, Dornhofer N, Kong C, Le QT, et al. Lysyl oxidase is essential for hypoxia-induced metastasis. *Nature* 2006; 440: 1222-1226.

[10] Sion AM, Figg WD. Lysyl oxidase (LOX) and hypoxia-induced metastases. *Cancer Biol Ther* 2006; 5(8): 909-11.

[11]Erler JT, Weaver VM. Three dimensional context regulation of metastasis. *Clin Exp Metastasis* 2009; 26: 35-49.

[12] Baker HE, Cox TR, and Erler JT. The rationale for targeting the LOX family in cancer. *Nat Rev*

Cancer 2012; 12(8): 540-552

[13] Kagan HM, Li W. Lysyl oxidase: properties, specificity, and biological roles inside and outside of the cell. *J Cell Biochem* 2003; 88(4): 660-72.

[14] Baker AM, Cox TR, Bird D, Lang G, Murray GI, Sun XF, et al. The role of lysyl oxidase in SRC-dependent proliferation and metastasis of colorectal cancer. *J Natl Cancer Inst* 2011; 103: 407-424.

[15] Cox TR, Erler JT. Lysyl oxidase in colorectal cancer. *Am J Physiol Gastrointest Liver Physiol* 2013; 305: G659-G666.

[16] Xiao Q, and Ge G. Lysyl oxidase extracellular matrix remodeling and cancer metastasis. *Cancer Microenviron* 2012; 5: 261-273.

[17] Tammali R, Saxena A, Srivastava SK, Ramana KV. Aldose reductase inhibition prevents hypoxia-induced increase in hypoxia-inducible factor-1α (HIF-1α) and vascular endothelial growth factor (VEGF) by regulating 26 S proteasome-mediated protein degradation in human colon cancer cells. *J Biol Chem* 2011; 286: 24089-24100.

[18] Voloshenyuk TG, Landesman ES, Khoutorova E, Hart AD, Gardner JD. Induction of cardiac fibroblast lysyl oxidase by TGF-β1 requires PI3K/Akt, Smad3, and MAPK signaling. *Cytokine* 2011; 55: 90-97.

[19] Salceda S, Caro J. Hypoxia-inducible factor 1alpha (HIF-1alpha) protein is rapidly degraded by the ubiquitin-proteasome system under normoxic conditions. Its stabilization by hypoxia depends on redox-induced changes. *J Biol Chem.* 1997; 272(36): 22642-7.

[20] Alam H, Maizels ET, Park Y, Ghaey S, Feiger ZJ, Chandel NS, Hunzicker-Dunn M. Follicle-stimulating hormone activation of hypoxia-inducible factor-1 by the phosphatidylinositol 3-kinase/AKT/Ras homolog enriched in brain (Rheb)/mammalian target of rapamycin (mTOR) pathway is necessary for induction of select protein markers of follicular differentiation. *J Biol Chem.* 2004; 279(19): 19431-40.

[21] Land SC, Tee AR. Hypoxia-inducible factor 1α is regulated by the mammalian target of rapamycin (mTOR) via an mTOR signaling motif. *J Biol Chem.* 2007; 282(28): 20534-43.

[22] Shi GX, Andres DA, Cai W. Ras family small GTPase-mediated neuroprotective signaling in stroke. *Cent Nerv Syst Agents Med Chem* 2011; 11(2): 114-37.

[23] Chan DA, Sutphin PD, Denko NC, and Giaccia AJ. Role of prolyl hydroxylation in oncogenically stabilized hypoxia-inducible factor-1α. *J Biol Chem* 2002; 277: 40112–40117.

[24] Blancher C, Moore JW, Robertson N, Harris AL. Effects of ras and von Hippel-Lindau (VHL) gene mutations on hypoxia-inducible factor (HIF)-1α, HIF-2α, and vascular endothelial growth factor expression and their regulation by the phosphatidylinositol 3′-kinase/Akt signaling pathway. *Cancer Res* 2001; 61(19): 7349–7355.

[25] Kikuchi H, Pino MS, Zeng M, Shirasawa S, Chung DC. Oncogenic KRAS and BRAF differentially regulate hypoxia-inducible factor-1α and -2α in colon cancer. *Cancer Res* 2009; 69(21): 8499–8506.

[26] Yoshikawa Y, Satoh T, Tamura T, Wei P, Bilasy SE, Edamatsu H., et al. The M-Ras-RA-GEF-2-Rap1 pathway mediates tumor necrosis factor-α-dependent regulation of integrin activation in splenocytes. *Mol Biol Cell* 2007; 18: 2949-2959.

[27] Denko NC, Fontana LA, Hudson KM, Sutphin PD, Raychaudhuri S, Altman R, et al. Investigating hypoxic tumor physiology through gene expression patterns. *Oncogene* 2003; 22: 5907-5914.

[28] Fu Beibei, Xue Jing, Li Zhaodong, Shi Xianglin, Jiang Bing-Hua, and Fang Jing. Chrysin inhibits expression of hypoxia-inducible factor-1α through reducing hypoxia-inducible factor-1α stability and inhibiting its protein synthesis. *Mol Cancer Ther* 2007; 6(1): 220-226.

[29] Li L, Xiong Y, Qu Y, Mao M, Mu W, Wang H, Mu D. The requirement of extracellular signal-related protein kinase pathway in the activation of hypoxia inducible factor 1α in the developing rat brain after hypoxia-ischemia. *Acta Neuropathol* 2008; 115(3): 297–303.

[30] Crespo S, Kind M, Arcaro A. The role of the PI3K/AKT/mTOR pathway in brain tumor metastasis.

J Cancer Metastasis Treat 2016; 2: 80-9.

[31] Xue G, Restuccia DF, Lan Q, Hynx D, Dirnhofer S, Hess D, Rüegg C, Hemmings BA. Akt/PKB-mediated phosphorylation of Twist1 promotes tumor metastasis via mediating cross-talk between PI3K/Akt and TGF-β signaling axes. *Cancer Discov* 2012; 2: 248-59.

[32] Ruvolo PP. GSK-3 as a novel prognostic indicator in leukemia. *Adv Biol Regul.* 2017; pii: S2212-4926(17)30086-6.

[33] Liu P, Cheng H, Roberts TM, Zhao JJ. Targeting the phosphoinositide 3-kinase pathway in cancer. *Nat Rev Drug Discov* 2009; 8: 627-644.

[34] Cox TR, Bord D, Baker AM, Baker HE, Ho MW, Lang G, et al. Lox-mediated collagen crosslinking is responsible for fibrosis-enhanced metastasis. *Cancer Res* 2012; 73: 1721-1732.

[35] Levental KR, Yu H, Kass L, Lakins JN, Egeblad M, Erler JT, et al. Matrix crosslinking forces tumor progression by enhancing integrin signaling. *Cell* 2009; 139: 891-906.

[36] Baker AM, Bird D, Lang G, Cox TR, Erler JT. Lysyl oxidase exzymatic function increases stiffness to drive colorectal cancer progression through FAK. *Oncogene* 2013; 32: 1863-1868.

[37] Ghosh S, Spagnoli GC, Martin I, Ploegert S, Demougin P, Heberer M, *et al*. Three-dimensional culture of melanoma cells profoundly affects gene expression profile: a high density oligonucleotide array study. *J Cell Physiol* 2005; 204(2): 522-31.

[38] Gill BJ and West JL. Modeling the tumor extracellular matrix: Tissue engineering tools repurposed towards new frontiers in cancer biology. *J Biomech* 2014; 47(9): 1969-78.

[39] Ohsawa S, Sato Y, Enomoto M, Nakamura M, Betsumiya A, Igaki T. Mitochondrial defect drives non-autonomous tumour progression through Hippo signaling in Drosophila. *Nature* 2012; 490(7421): 547-551.

[40] Kamphorst JJ, Cross JR, Fan J, Stanchina E, Mathew R, White EP. Hypoxic and Ras-transformed cells support growth by scavenging unsaturated fatty acids from lysophospholipids. *Proc Natl Acad Sci*

USA 2013; 110: 8882-8887.

[41] Masgras I, Ciscato F, Brunati AM, Tibaldi E, Indraccolo S, and Curtarello M, et al. Absence of Neurofibromin Induces an Oncogenic Metabolic Switch via Mitochondrial ERK-Mediated Phosphorylation of the Chaperone TRAP1. *Cell Rep*. 2017 Jan 17; 18(3): 659-672.

Legends to Figures

Figure 1. Crucial role of Ras in LOX expression. A. Lysates of the indicated cells in 2D culture, treated with Kobe0065 (*65*) or the vehicle DMSO (*D*), were subjected to the detection of prepro-LOX and GAPDH by western blotting with the anti-LOX and anti-GAPDH antibodies, respectively. **B.** Twenty-four hours after transfection of LOX siRNA (*L*), K-Ras siRNA (*K*) or the non-targeting control RNA (*ctrl*), the indicated cells in 2D culture were treated with Kobe0065 (*65*) or DMSO (*D*) as described in *Materials and Methods*. Thereafter, total RNAs were prepared and subjected to the measurements of the relative *LOX* and K-*ras* mRNA levels by qRT-PCR using the *GAPDH* mRNA levels as an internal control. Three independent experiments, each conducted in triplicate, yielded essentially equivalent results. **C.** Lysates of the cells, treated as in *B*, were subjected to the detection of prepro-LOX and GAPDH as described in *A*. **D.** Twenty-four hours after transfection of LOX siRNA (*L*), K-Ras siRNA (*K*) or the control RNA (*ctrl*), the indicated cells in 3D culture were treated with Kobe0065 (*65*) or DMSO (*D*) and subjected to the measurements of the relative *LOX* and K-*ras* mRNA levels as described in *B*. Three independent experiments, each conducted in triplicate, yielded essentially equivalent results. **E.** Lysates of the cell, treated as in *D*, were subjected to the detection of prepro-LOX and GAPDH by western blotting as described in *A*. **F.** NIH3T3 cells (*NIH*) and those stably expressing H-Ras^{G12V} (*NIH/H*) in 2D (*left panel*) or 3D *(right panel*) culture were treated with Kobe0065 (*65*) or DMSO (*D*) and subjected to the measurements of the relative *LOX* and K-*ras* mRNA levels as described in *B*. Four independent experiments, each conducted in triplicate, yielded essentially equivalent results. **G.** Lysates of the cells, treated as in *F*, were subjected to the detection of prepro-LOX and GAPDH by western blotting as described in *A*. **H.** NIH3T3 cells stably expressing H-Ras^{G12V} (*NIH/H*) in 3D culture were treated with Kobe0065 (*65*) or DMSO (*D*) as described in *B*. The culture media were subjected to immunoprecipitation with the anti-LOX antibody and Protein A-Sepharose at 4 °C overnight, and secreted mature-LOX in the immunoprecipitates was detected by western blotting with the anti-LOX

antibody. On the other hand, lysates of the cells were subjected to detection of GAPDH by the anti-GAPDH antibody.

Numbers below the lanes in *A*, *C*, *E*, *G* and *H* indicate the values of prepro-LOX/GAPDH relative to those of the DMSO-treated cells. Numbers below the lanes in *F* indicate the values of prepro-LOX/GAPDH relative to those of the DMSO-treated cells in 2D culture. Statistical analysis was performed as described in *Materials and Methods*.

Figure 2. Crucial role of the PI3K-Akt signaling in Ras-mediated LOX expression. A. Twenty-four hours after transfection of K-Ras siRNA (*K*) or the non-targeting control (*ctrl*), SW620 cells in 3D culture were treated with Kobe0065 (*65*), LY294002 (*LY*) or DMSO (*D*) as described in *Material & Methods*. Thereafter, total RNAs were prepared and subjected to the measurements of the relative *LOX* and K-*ras* mRNA levels by qRT-PCR using the *GAPDH* mRNA levels as an internal control. Three independent experiments, each conducted in triplicate, yielded essentially equivalent results. **B.** Lysates of the cells, treated as in *A*, were subjected to the detection of prepro-LOX, phosphorylated Akt (*p*), total Akt (*t*) and GAPDH by western blotting with the respective antibodies. **C.** SW620 and MCF-7 cells in 3D culture were treated with Kobe0065 (*65*) or DMSO (*D*) and subjected to the detection of prepro-LOX, phosphorylated Akt (*p*), total Akt (*t*) and GAPDH by western blotting as described in *B*. **D.** NIH3T3 cells (*NIH*) and those stably expressing H-Ras^{G12V} (*NIH/H*) in 3D culture were treated with Kobe0065 (*65*), LY294002 (*LY*) or DMSO (*D*) and subjected to the measurements of the relative *LOX* and K-*ras* mRNA levels as described in *A*. Three independent experiments, each conducted in triplicate, yielded essentially equivalent results. **E.** Lysates of the cells, treated as in *D*, were subjected to the detection of prepro-LOX, phosphorylated Akt (*p*), total Akt (*t*) and GAPDH by western blotting as described in *B*. **F.** NIH3T3 cells (*N*) and those stably expressing H-Ras^{G12V} (*N/H*) or c-Raf$^{S259A,\ Y340D,\ Y341D}$ (N/R) in 3D culture were treated with Kobe0065 (*65*) or DMSO (*D*) and subjected to the measurements of the relative *LOX* mRNA levels by qRT-PCR using the *β-actin* mRNA levels as an

internal control as described in *A*. Three independent experiments, each conducted in duplicate, yielded essentially equivalent results.

Numbers below the lanes in *B*, *C* and *E* indicate the values of prepro-LOX/GAPDH and phosphorylated Akt/total Akt relative to those of the DMSO-treated cells. Numbers below the lanes in *D* and *F* indicate the values of the *LOX*/*GAPDH* and the *LOX*/*β-actin* mRNAs, respectively, relative to those of the DMSO-treated NIH3T3 cells. Statistical analysis was performed as described in *Materials and Methods*.

Figure 3. Crucial role of HIF-1α protein accumulation in Ras-PI3K-Akt-mediated LOX expression. A. Twenty-four hours after transfection of K-Ras siRNA (*K*) or the non-targeting control (*ctrl*), SW620 cells in 3D culture were treated with Kobe0065 (*65*), LY294002 (*LY*), β-APN (*β*) or DMSO (*D*) as described in *Material & Methods*. Thereafter, total RNAs were prepared and subjected to the measurements of the relative mRNA levels of *LOX*, K-*ras* and *HIF-1α* by qRT-PCR using the *GAPDH* mRNA levels as an internal control. Three independent experiments, each conducted in triplicate, yielded essentially equivalent results. **B.** Lysates of the cells, treated as in *A*, were subjected to the detection of HIF-1α, prepro-LOX, phosphorylated Akt (*p*), total Akt (*t*) and GAPDH by western blotting with the respective antibodies. **C.** NIH3T3 cells (*NIH*) and those stably expressing H-Ras^{G12V} (*NIH/H*) in 3D culture were treated with Kobe0065 (*65*), LY294002 (*LY*), β-APN (*β*) or DMSO (*D*) and subjected to the measurements of the relative *HIF-1α* mRNA levels as described in *A*. Three independent experiments, each conducted in triplicate, yielded essentially equivalent results. **D.** Lysates of the cells, treated as in *C*, were subjected to the detection of HIF-1α, prepro-LOX, phosphorylated Akt (*p*), total Akt (*t*) and GAPDH by western blotting as described in *B*. **E.** SW620 and NIH3T3 cells stably expressing H-Ras^{G12V} (NIH/H) in 3D cell culture were treated with Kobe0065 (*65*), Chrysin (*C*) or DMSO (*D*) and subjected to the measurements of the relative *HIF-1α* mRNA levels as described in *A*. Three independent experiments, each conducted in triplicate, yielded essentially equivalent results. **F.**

Lysates of the cells, treated as in *E*, were subjected to the detection of HIF-1α, prepro-LOX, phosphorylated Akt (*p*), total Akt (*t*) and GAPDH by western blotting as described in *B*.

Numbers below the lanes in *B*, *D* and *F* indicate the values of HIF-1α, prepro-LOX/GAPDH and phosphorylated Akt/total Akt relative to those of the DMSO-treated cells. Statistical analysis was performed as described in *Materials and Methods*.

Figure 4. Inhibition of migration of cancer cells carrying the active *ras* mutations by Kobe0065. A. Twenty-four hours after transfection of K-Ras siRNA (*K*), LOX siRNA (*L*) or the non-targeting control (*ctrl*), the indicated cells were treated with Kobe0065 (*65*), LY294002 (*LY*), β-APN (*β*) or DMSO (*D*) and subjected to the wound healing migration assay as described in *Material & Methods*. Shown are photographs of the cells migrated into the wounded areas 24 h for SW620 and Panc-1 and 48 h for BxPC-3 after the wounds were generated. **B.** Twenty-four hours after the transfection of various siRNAs as described in *A*, the cells were subjected to the anchorage-dependent proliferation assay in the presence of Kobe0065 (*65*) or DMSO (*D*) for 72 h as described in *Materials and Methods*. All the experiments, each consisting of 8 wells, were performed 3 times.

Figure 5. Inhibition of invasion of cancer cells carrying the active *ras* mutations by Kobe0065. A. The Matrigel™ cell invasion assay was carried out on SW620, Panc-1 and BxPC-3 cells in the presence of the indicated concentrations of Kobe0065 or DMSO as described in *Materials and Methods*. Shown are photographs of the hematoxylin-stain of the cells invaded into the membranes after incubation for 24 h. **B.** Relative number of the invading cells. The numbers of the invaded cells in 3 chambers for each point were counted and normalized to those of the DMSO-treated cells. Statistical analysis was performed as described in *Materials and Methods*.

Figure 6. Inhibition of lung metastasis of SW620 cells by oral administration of Kobe0065. Nude mice were orally administered with the indicated doses of Kobe0065 or sorafenib for 5 consecutive days. Subsequently, 1×10^7 SW620 cells were injected via tail vein and the oral administration was continued

for further 8 weeks (5 days/week) as described in *Materials and Methods*. Thereafter, the numbers of micro-metastatic nodules in the dissected lungs were counted under a microscope on the H&E-stained sections as described in *Materials and Methods*. **A.** The numbers and ratios of mice carrying the lung metastatic nodules. **B.** Representative photographs of the frontal sections of the lungs subjected to H&E-staining. Arrows indicate metastatic tumor nodules. **C.** The numbers of the metastatic nodules per lung. **D.** Total RNAs were prepared from the lung sections described in *B* and subjected to the measurement of the relative *LOX* mRNA levels by qRT-PCR using the *GAPDH* mRNA levels as an internal control as described in *Materials and Methods*. Three independent experiments, each conducted in triplicate, yielded essentially equivalent results. Statistical analysis was performed as described in *Materials and Methods*. **E.** The lung sections described in *B* were subjected to immunohistochemical detection of LOX by the anti-LOX antibody (Santa Cruz Biotech.) and the horseradish peroxidase-conjugated secondary antibody against rabbit immunoglobulin G. Shown are the immunostained images of the boxed regions in *B*, where immunoreactive signals were shown by a brown color.

Fig. 1

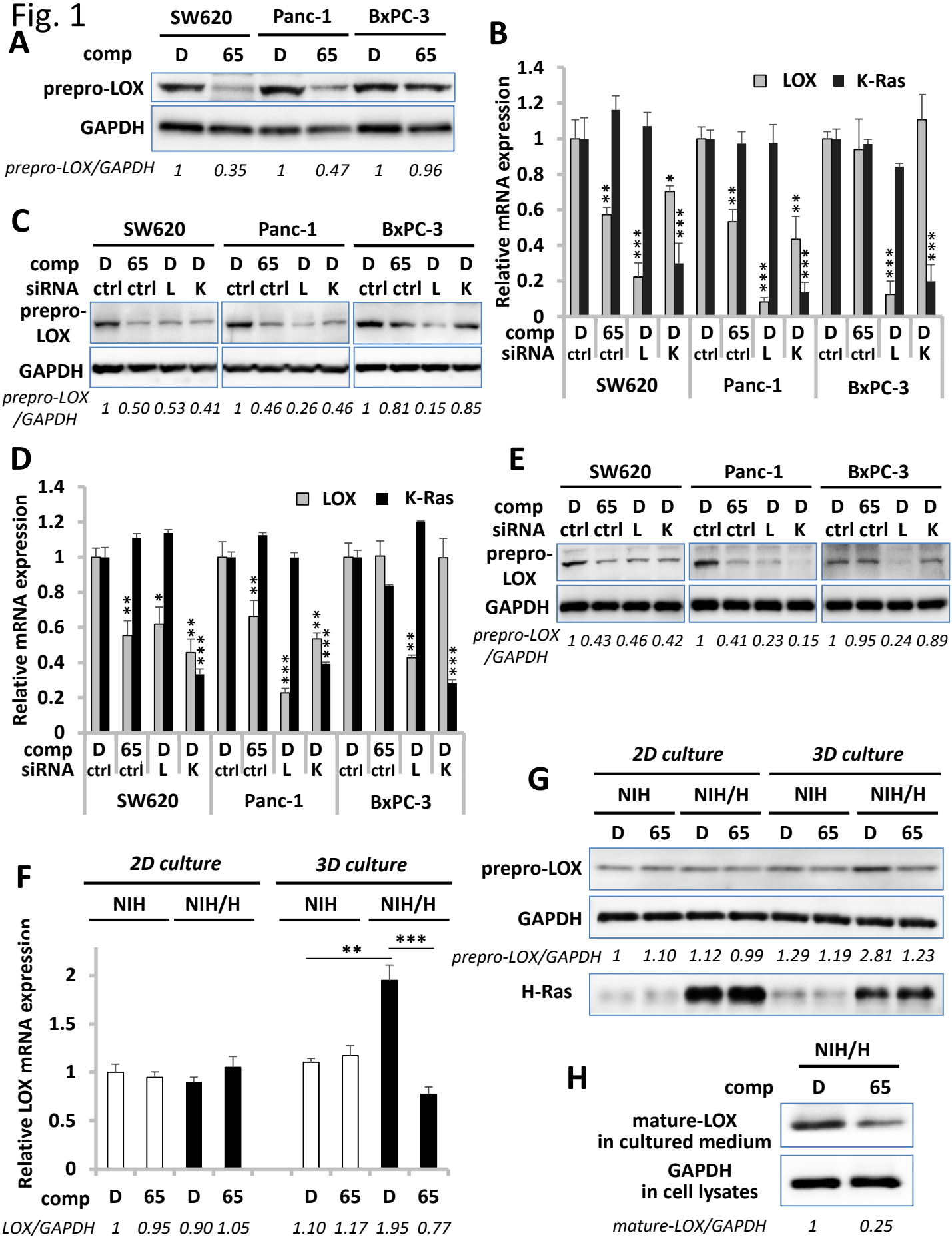
A
SW620
Panc-1
BxPC-3
comp
D
65
prepro-LOX
GAPDH
prepro-LOX/GAPDH
1 0.35 1 0.47 1 0.96
B
LOX
K-Ras
Relative mRNA expression
comp
siRNA
ctrl
L
K
SW620
Panc-1
BxPC-3
C
prepro-LOX
GAPDH
prepro-LOX /GAPDH
1 0.50 0.53 0.41 1 0.46 0.26 0.46 1 0.81 0.15 0.85
D
LOX
K-Ras
Relative mRNA expression
E
prepro-LOX
GAPDH
prepro-LOX /GAPDH
1 0.43 0.46 0.42 1 0.41 0.23 0.15 1 0.95 0.24 0.89
F
2D culture
3D culture
NIH
NIH/H
Relative LOX mRNA expression
LOX/GAPDH
1 0.95 0.90 1.05 1.10 1.17 1.95 0.77
G
2D culture
3D culture
NIH
NIH/H
prepro-LOX
GAPDH
prepro-LOX/GAPDH
1 1.10 1.12 0.99 1.29 1.19 2.81 1.23
H-Ras
H
NIH/H
comp
D
65
mature-LOX in cultured medium
GAPDH in cell lysates
mature-LOX/GAPDH
1 0.25

Fig.2

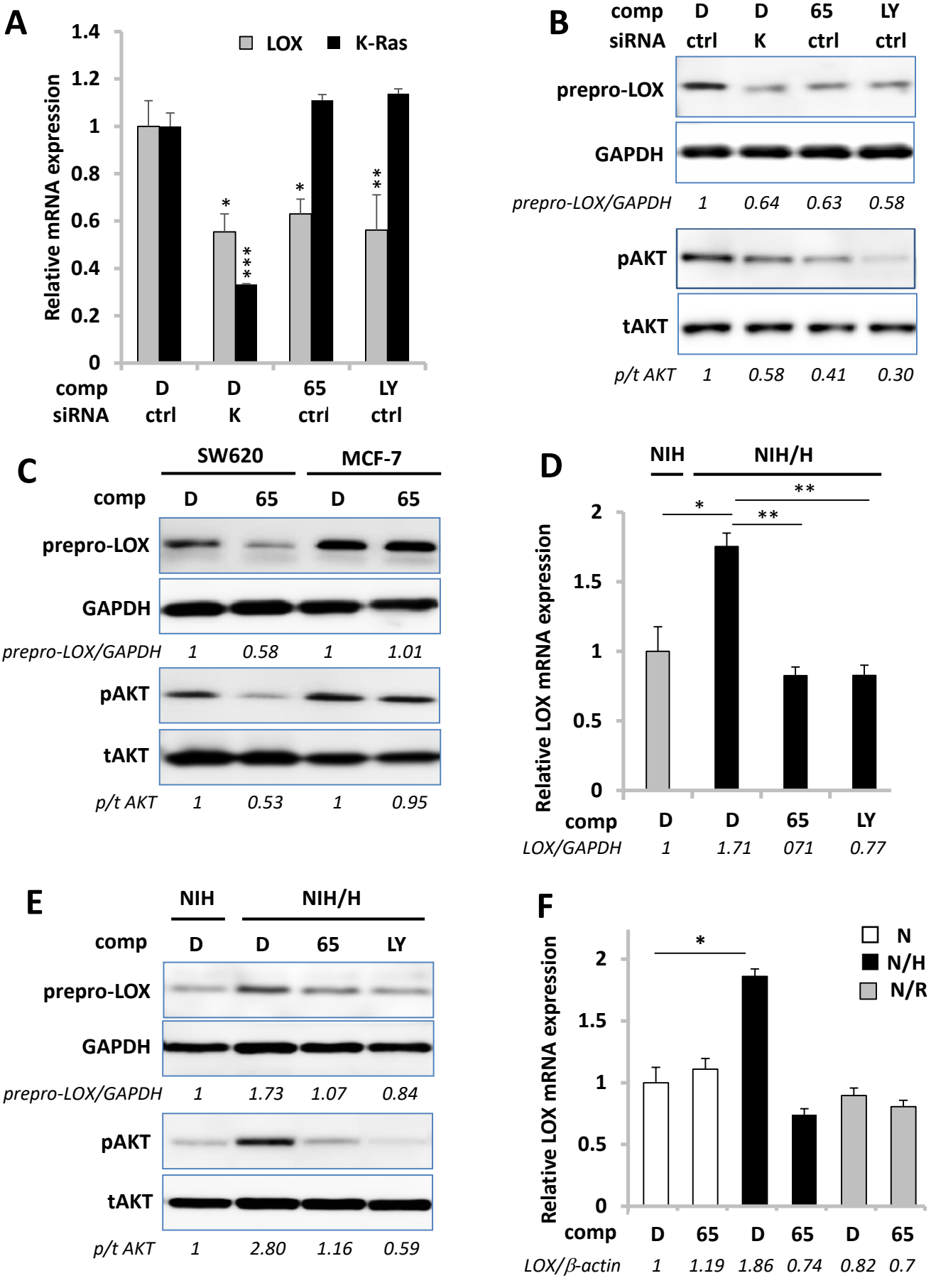
A
LOX
K-Ras
Relative mRNA expression
1.4
1.2
1
0.8
0.6
0.4
0.2
0
comp D D 65 LY
siRNA ctrl K ctrl ctrl
B
comp D D 65 LY
siRNA ctrl K ctrl ctrl
prepro-LOX
GAPDH
prepro-LOX/GAPDH 1 0.64 0.63 0.58
pAKT
tAKT
p/t AKT 1 0.58 0.41 0.30
C
SW620
MCF-7
comp D 65 D 65
prepro-LOX
GAPDH
prepro-LOX/GAPDH 1 0.58 1 1.01
pAKT
tAKT
p/t AKT 1 0.53 1 0.95
D
NIH
NIH/H
Relative LOX mRNA expression
2
1.5
1
0.5
0
comp D D 65 LY
LOX/GAPDH 1 1.71 071 0.77
E
NIH
NIH/H
comp D D 65 LY
prepro-LOX
GAPDH
prepro-LOX/GAPDH 1 1.73 1.07 0.84
pAKT
tAKT
p/t AKT 1 2.80 1.16 0.59
F
N
N/H
N/R
Relative LOX mRNA expression
2
1.5
1
0.5
0
comp D 65 D 65 D 65
LOX/β-actin 1 1.19 1.86 0.74 0.82 0.7

Fig. 3

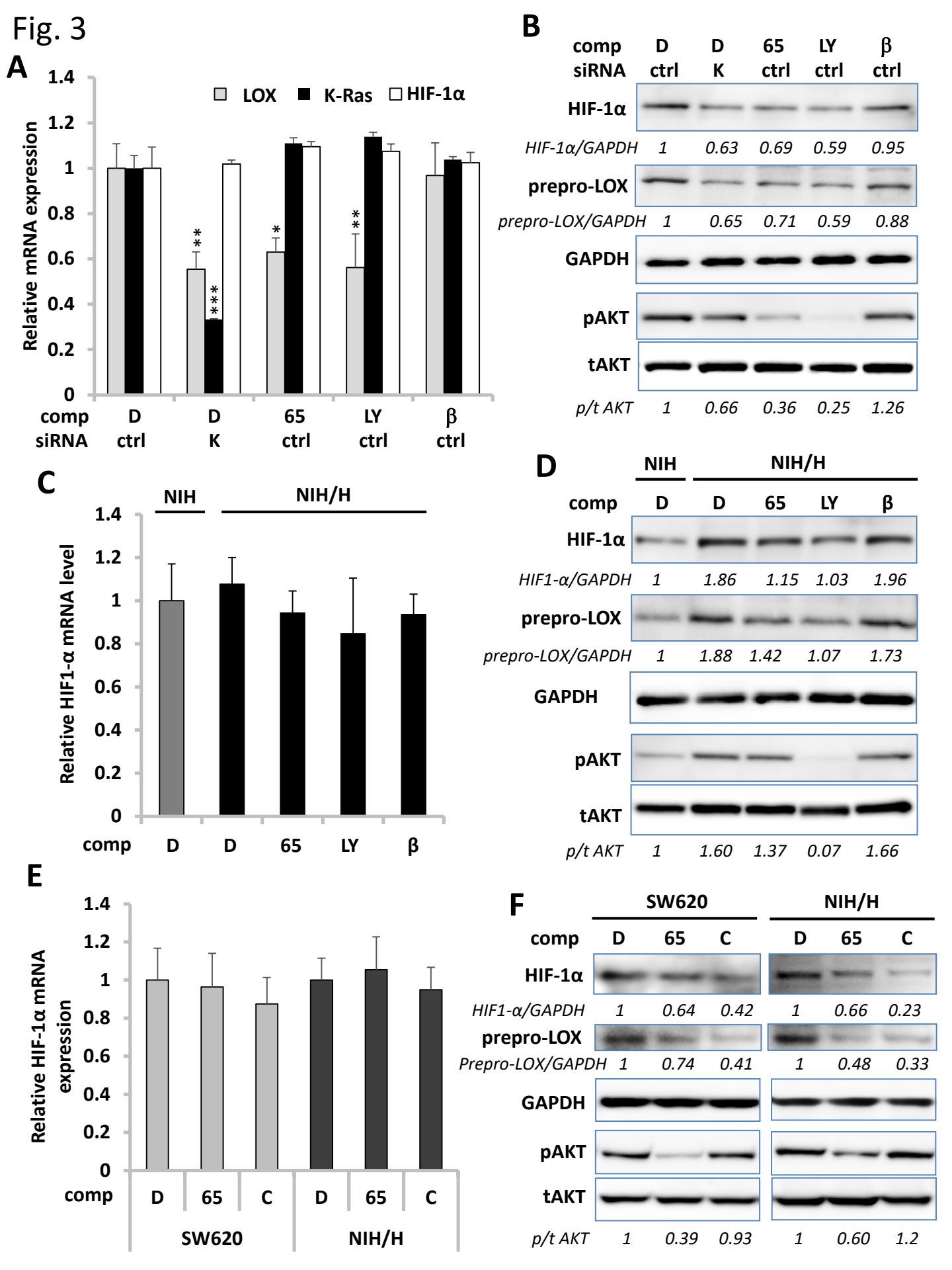
A
LOX
K-Ras
HIF-1α
Relative mRNA expression
comp
siRNA
D ctrl
D K
65 ctrl
LY ctrl
β ctrl
B
comp
siRNA
HIF-1α
HIF-1α/GAPDH 1 0.63 0.69 0.59 0.95
prepro-LOX
prepro-LOX/GAPDH 1 0.65 0.71 0.59 0.88
GAPDH
pAKT
tAKT
p/t AKT 1 0.66 0.36 0.25 1.26
C
NIH
NIH/H
Relative HIF1-α mRNA level
comp
D
D
65
LY
β
D
NIH
NIH/H
comp
HIF-1α
HIF1-α/GAPDH 1 1.86 1.15 1.03 1.96
prepro-LOX
prepro-LOX/GAPDH 1 1.88 1.42 1.07 1.73
GAPDH
pAKT
tAKT
p/t AKT 1 1.60 1.37 0.07 1.66
E
Relative HIF-1α mRNA expression
comp
D
65
C
SW620
NIH/H
F
SW620
NIH/H
comp
HIF-1α
HIF1-α/GAPDH 1 0.64 0.42 1 0.66 0.23
prepro-LOX
Prepro-LOX/GAPDH 1 0.74 0.41 1 0.48 0.33
GAPDH
pAKT
tAKT
p/t AKT 1 0.39 0.93 1 0.60 1.2

Fig. 4

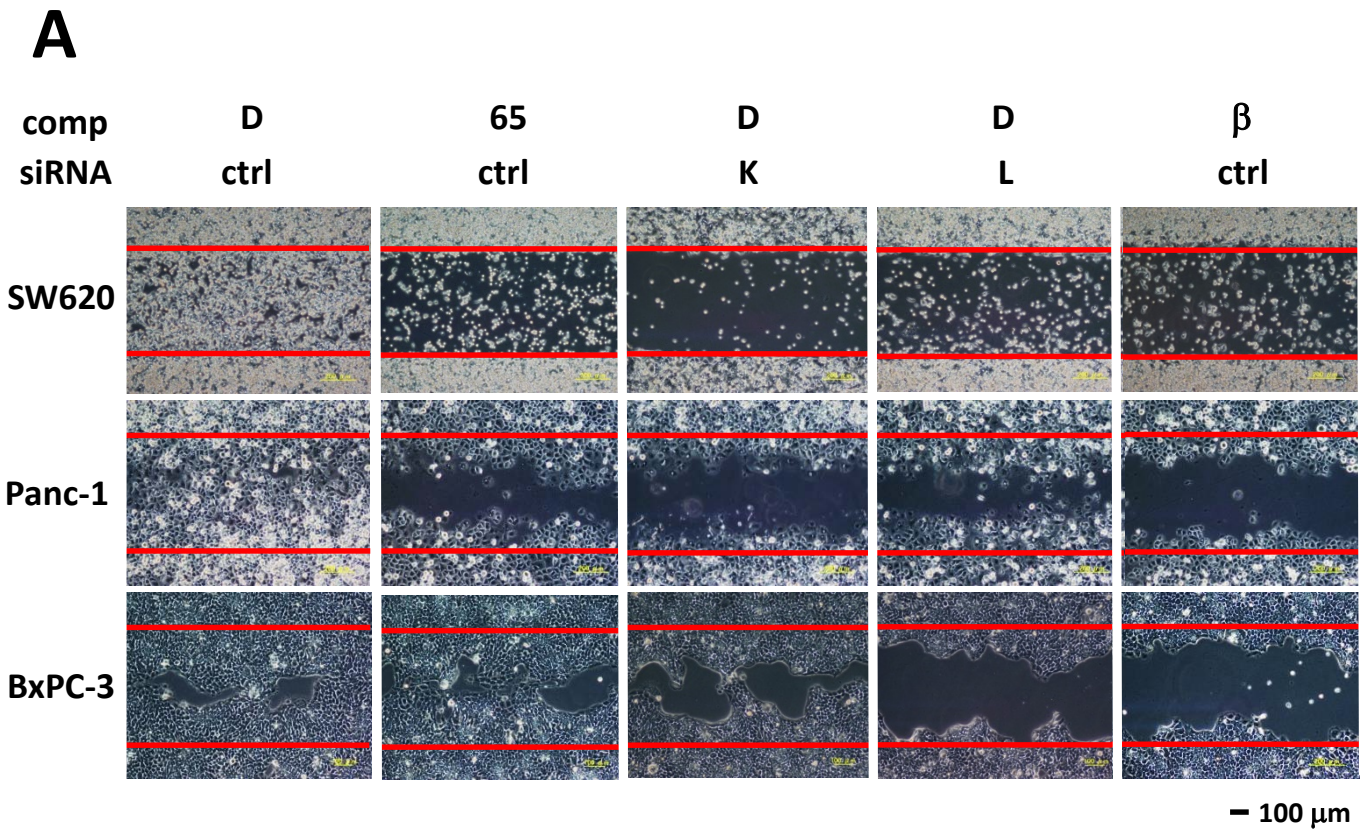
A
comp
siRNA
D
ctrl
65
ctrl
D
K
D
L
β
ctrl
SW620
Panc-1
BxPC-3
100 μm

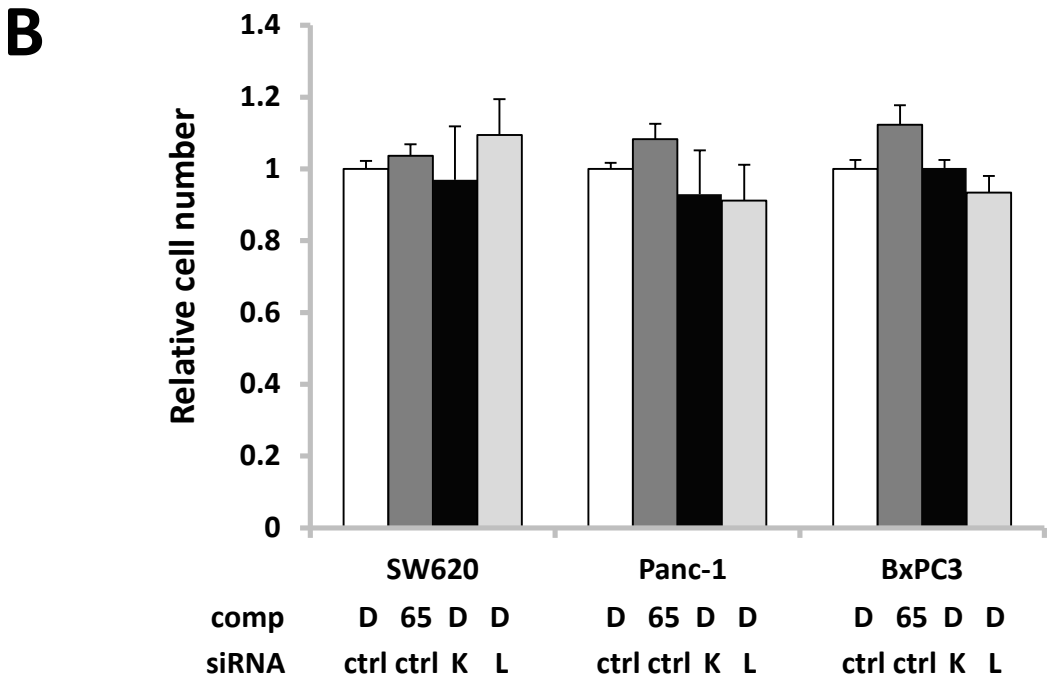
B
Relative cell number
1.4
1.2
1
0.8
0.6
0.4
0.2
0
SW620
Panc-1
BxPC3
comp
siRNA
D 65 D D
ctrl ctrl K L

Fig. 5

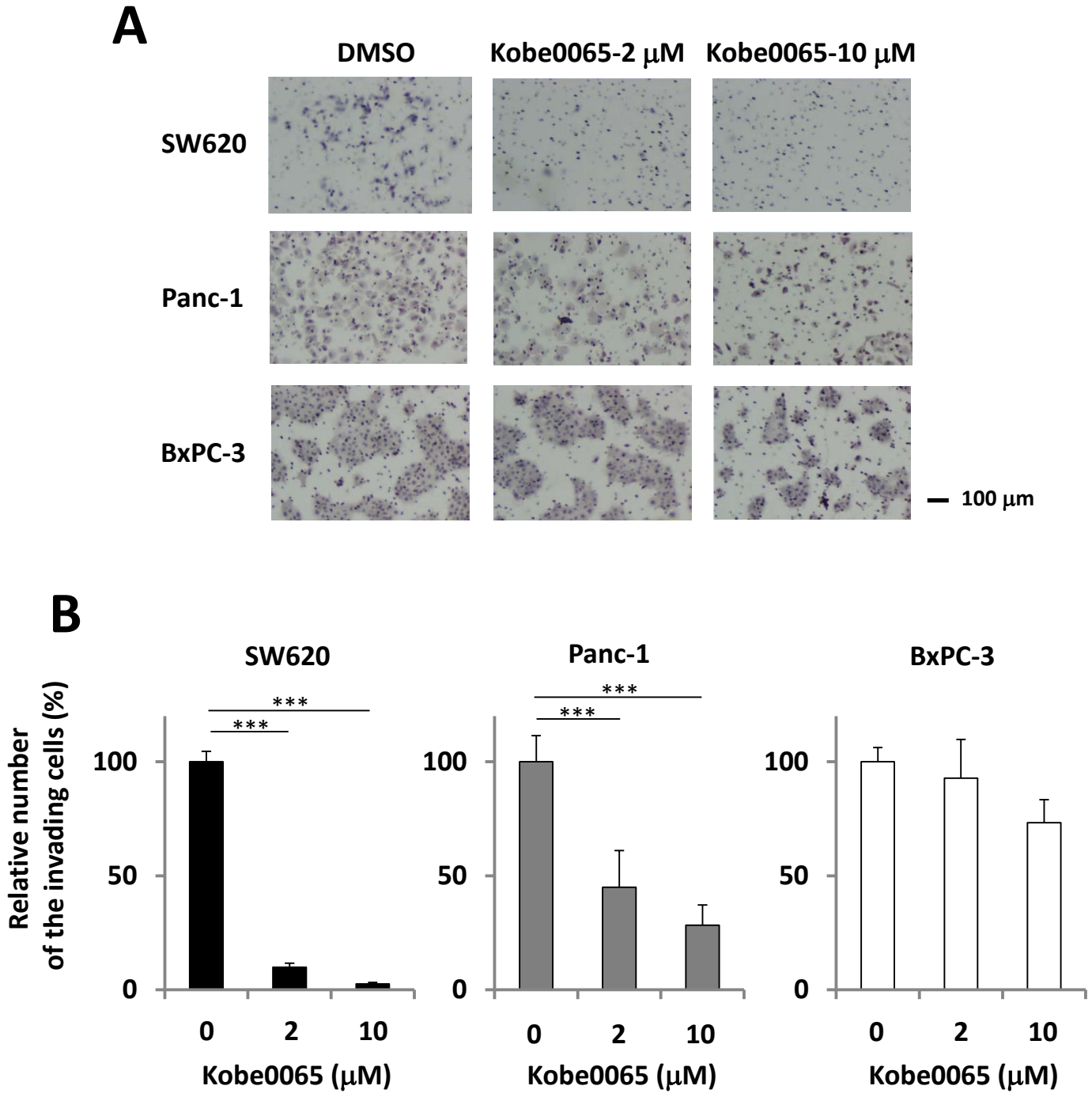
A
DMSO
Kobe0065-2 μM
Kobe0065-10 μM
SW620
Panc-1
BxPC-3
100 μm
B
SW620
Panc-1
BxPC-3
Relative number of the invading cells (%)
***
***
***
***
100
50
0
0
2
10
Kobe0065 (μM)

Fig. 6

A

Treatment	number of mice with metastasis
vehicle	7/7 (100%)
Kobe0065 80 mg/kg	3/4 (75%)
Kobe0065 160 mg/kg	3/6 (50%)
sorafenib 80 mg/kg	5/5(100%)

B

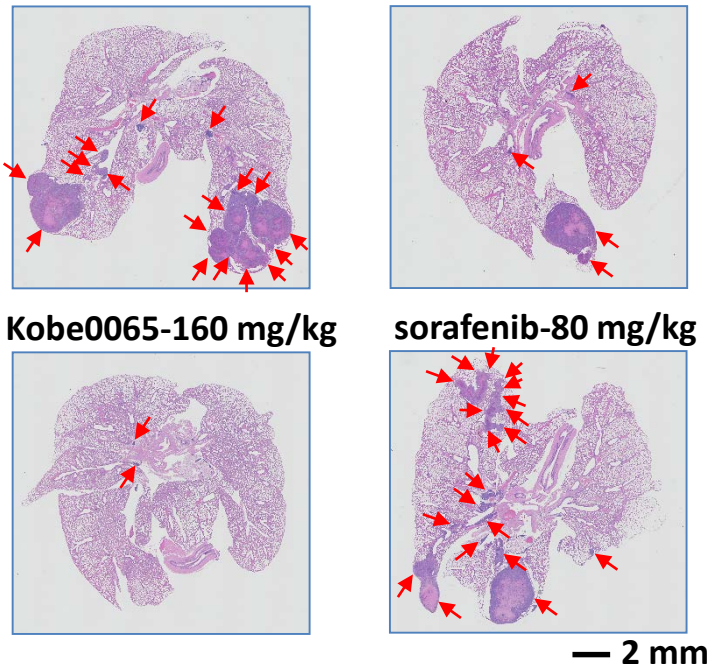

C

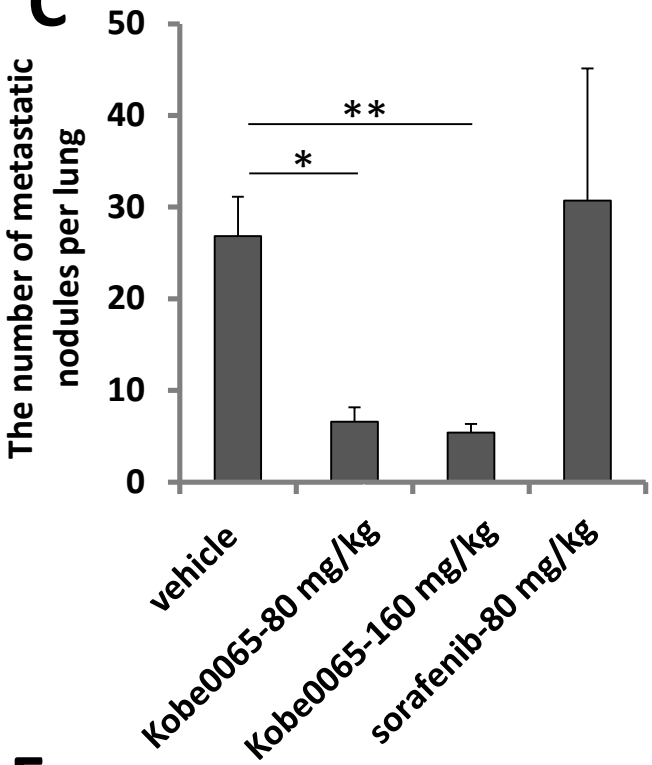

D

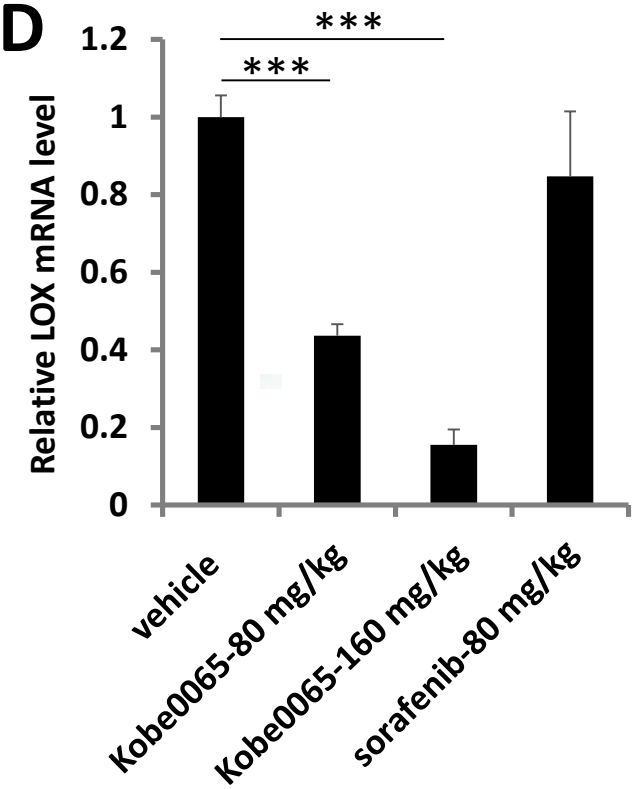

E

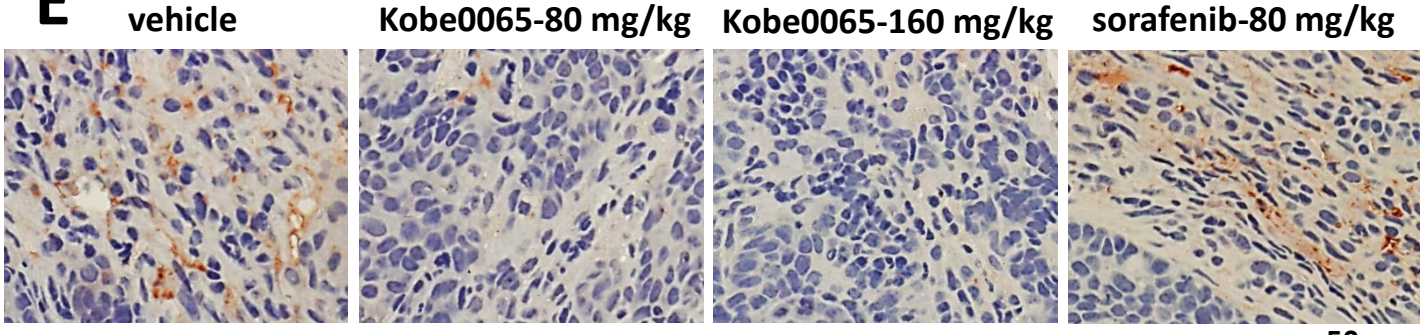

Yoshikawa Y, *et al*. Supplementary Fig. 1

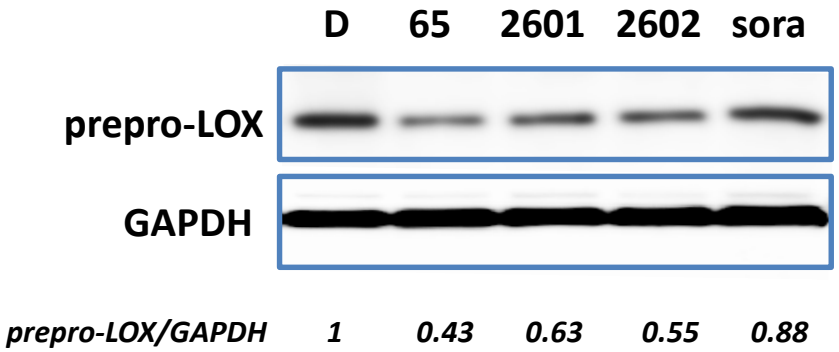

Effects of Kobe0065-family compounds on LOX expression. SW620 cells grown in 3D culture were treated with 20 μM Kobe0065 (65), 20 μM Kobe2601 (2601), 20 μM Kobe2602 (2602), 2 μM sorafenib (sora) or DMSO (D) as described in *Materials and Methods* and subjected to the detection of prepro-LOX and GAPDH by western blotting with the anti-LOX and anti-GAPDH antibodies, respectively. Numbers below the lanes indicate the values of prepro-LOX/GAPDH relative to those of the DMSO-treated cells.

Yoshikawa Y, *et al*. Supplementary Fig. 2

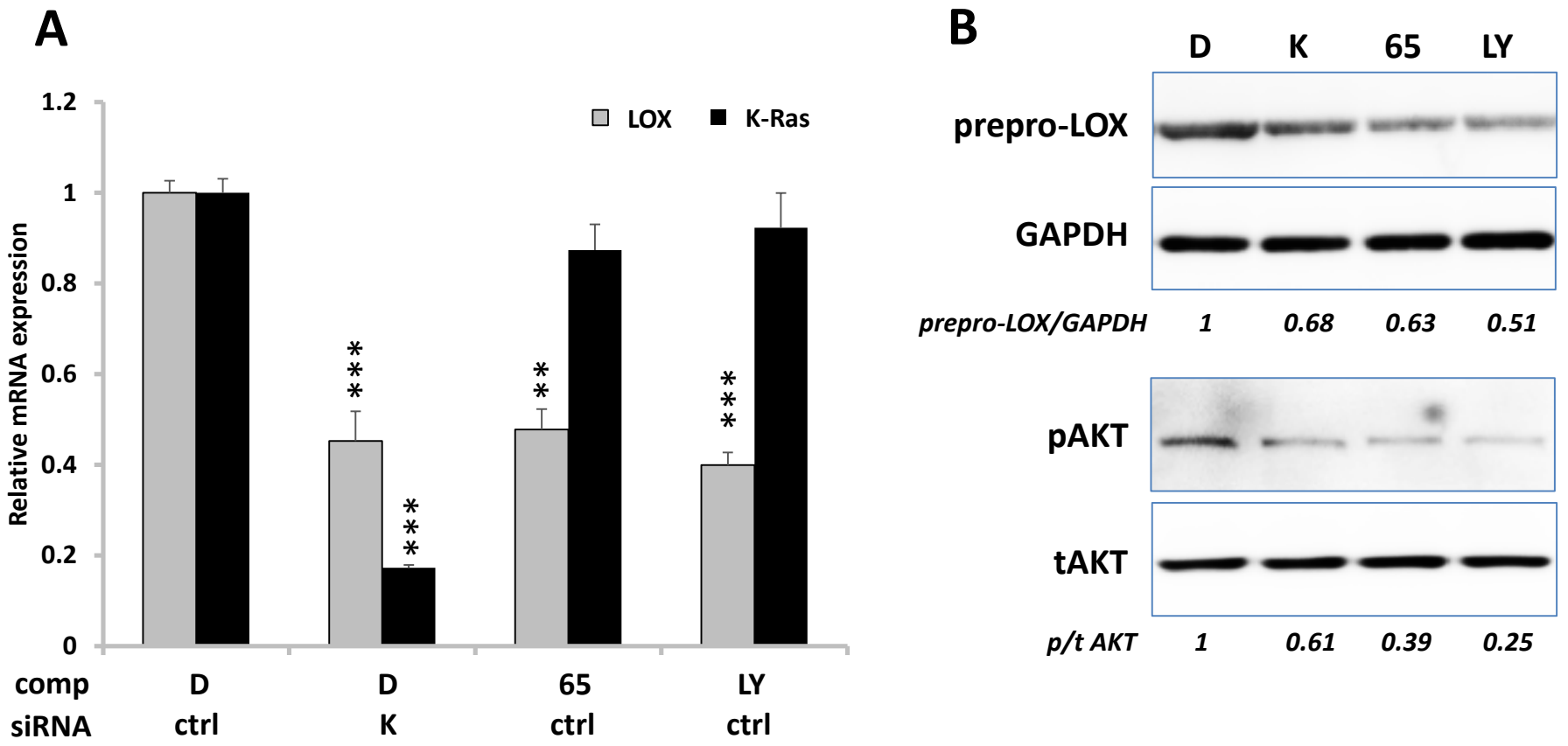

Crucial role of the PI3K-Akt signaling in Ras-mediated LOX expression in 2D-cultured SW620. A. SW620 cells in 2D culture were analyzed for the effects of the transfection of K-Ras siRNA (K) or the non-targeting control (ctrl) and of the treatments with Kobe0065 (65), LY294002 (LY) or DMSO (D) on the relative *LOX* and K-*ras* mRNA levels as described in Fig. 2A legend. Three independent experiments, each conducted in triplicate, yielded essentially equivalent results. **B.** Lysates of the cells, treated as described in *A*, were subjected to the detection of prepro-LOX, phosphorylated Akt (p), total Akt (t) and GAPDH by western blotting with the respective antibodies. Numbers below the lanes indicate the values of prepro-LOX/GAPDH and phosphorylated Akt/total Akt relative to those of the DMSO-treated cells.

Yoshikawa Y, *et al*. Supplementary Fig. 3

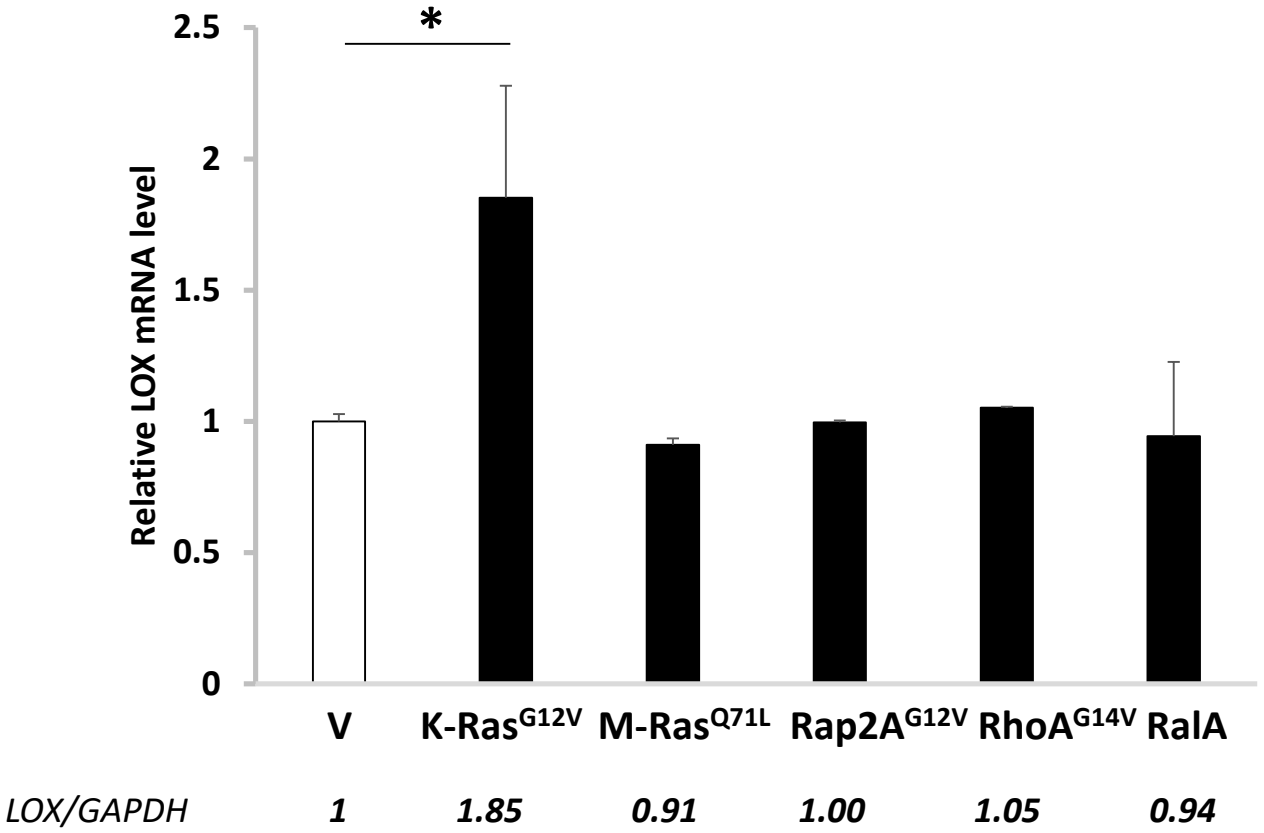

Effects of various small GTPases on LOX expression. NIH3T3 cells were transfected with pEF-BOS-HA vector (V), pEF-BOS-HA-K-Ras^{G12V} (K-Ras^{G12V}), pEF-BOS-HA-M-Ras^{Q71L} (M-Ras^{Q71L}), pEF-BOS-HA-Rap2A^{G12V} (Rap2A^{G12V}), pEF-BOS-HA-RhoA^{G14V} (RhoA^{G14V}) or pCMV2-flag-RalA (RalA) by using Lipofectoamine 2000 (Invitrogen) according to the manufacturer's instructions. Three days after transfection, total RNAs were prepared and subjected to the measurements of the relative *LOX* mRNA levels by qRT-PCR using the *GAPDH* mRNA levels as an internal control. Three independent experiments, each conducted in triplicate, yielded essentially equivalent results. Statistical analysis was performed as described in *Materials and Methods*.

Yoshikawa Y, *et al*. Supplementary Fig. 4

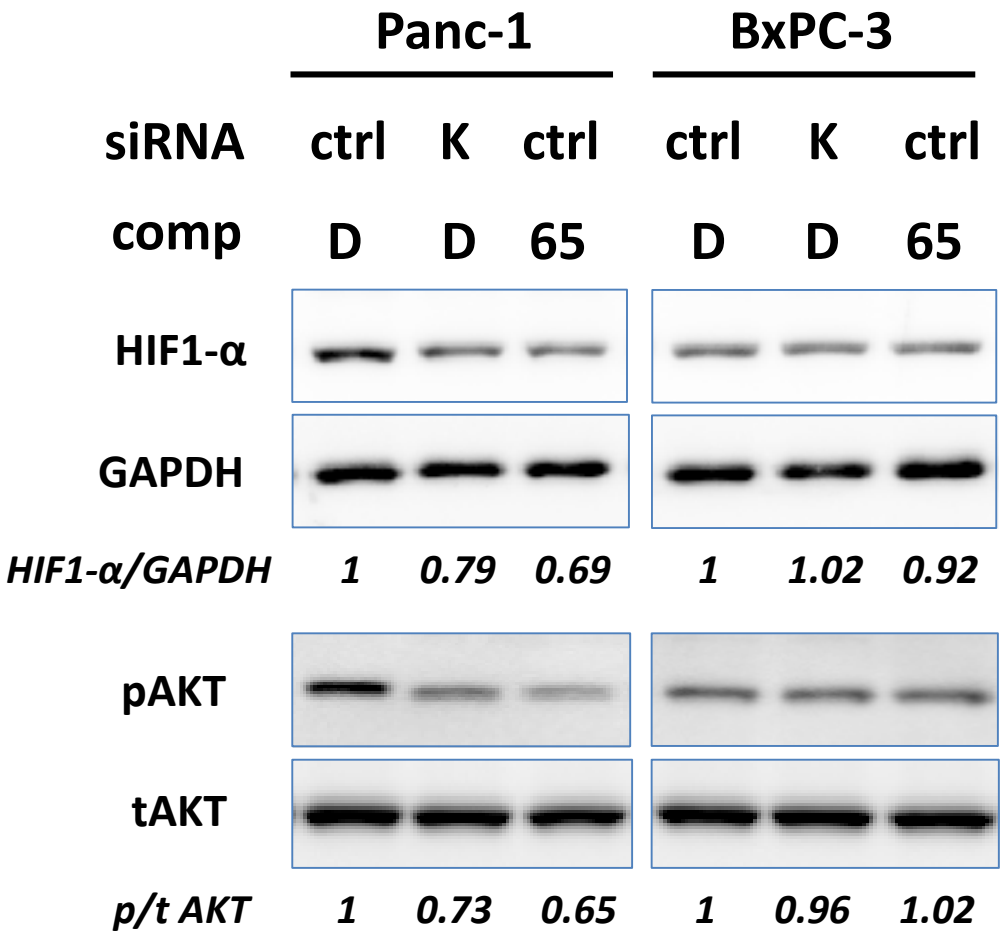

Role of Ras in accumulation of HIF-1α and Akt phosphorylation in Panc-1 and BxPC-3. Twenty-four hours after transfection of K-Ras siRNA (K) or the non-targeting control (ctrl), Panc-1 and BxPC-3 cells in 3D culture were treated with Kobe0065 (65) or DMSO (D) as described in *Material & Methods*. Thereafter, lysates of the cells were subjected to the detection of HIF-1a, GAPDH, phosphorylated Akt (p) and total Akt (t) by western blotting with the respective antibodies. Numbers below the lanes indicate the values of HIF-1α/GAPDH and phosphorylated Akt/total Akt relative to those of the DMSO-treated cells.

Supplementary Table 1. The nucleotide sequences of the Stealth siRNAs

Name	Species	Primer	Sequence
K-Ras	human	sense	5'-UGUGGACGAAUAUGAUCCAACAAUA-3'
		antisense	5'-UAUUGUUGGAUCAUAUUCGUCCACA-3'
		sense	5'-AUAACUUCUUGCUAAGUCCUGAGCC-3'
		antisense	5'-GGCUCAGGACUUAGCAAGAAGUUAU-3'
		sense	5'-CAAGACAGAGAGUGGAGGAUGCUUU-3'
		antisense	5'-AAAGCAUCCUCCACUCUCUGUCUUG-3'
LOX	human	sense	5'-AUCAUAAUCUCUGACAUCUGCCCUG-3'
		antisense	5'-CAGGGCAGAUCUCAGCACUUAUGAU-3'
		sense	5'-UGGGUAAGAAAUCUGAUGUCCCUUG-3'
		antisense	5'-CAAGGGACAUCAGAUUUCUUACCCA-3'
		sense	5'-GGAUUGAGUCCUGGCUGUUAUGAUA-3'
		antisense	5'-UAUCAUAACAGCCAGGACUCAAUCC-3'

Supplementary Table 2. Primers used for qRT-PCR

Name	Species	Primer	Sequence
LOX	mouse	forward	5’-TGCCAGTGGATTGATATTACAGATGT -3’
		reverse	5’-AGCGAATGTCACAGCGTACAA -3’
LOX	human	forward	5’-CCAGAGGAGAGTGGCT-3’
		reverse	5’-CCAGGTAGCTGGGGTT-3’
HIF-1α	mouse	forward	5’-CCCAGATTCAGGATCAGACAC -3’
		reverse	5’-TTGGATATAGGGAGCTAAC ATC-3’
HIF-1α	human	forward	5’-CCCAGATTCAGGATCAGACAC -3’
		reverse	5’-TTGGATATAGGGAGCTAAC ATC-3’
GAPDH	mouse	forward	5’-GAGATTGTTGCCATCAACGAC -3’
		reverse	5’-TTTGATGTTAGGGGGTCTCG -3’
GAPDH	human	forward	5’-CATCAATGGAAATCCCATCAC -3’
		reverse	5’-GCAGAGATGATGACCCTTTTG -3’
K-Ras	human	forward	5’-TGTGGTAGTTGGAGCTGGTG-3’
		reverse	5’-CCCAGTCCTCATGTACTGGTC -3’
β-actin	mouse	forward	5’-ATGAAGATCAAGATCATTGCTCCTC -3’
		reverse	5’-ACATCTGCTGGAAGGTGGACAG-3’